Electronic Supplementary Material (ESI) for Journal of Materials Chemistry C.

Supporting Information

Charge Generation Mechanism Tuned via Film Morphology in Small Molecule Bulk-Heterojunction Photovoltaic Materials

Sylvia J. Lou,[1] Stephen Loser,[1] Kyle A. Luck,[1] Nanjia Zhou,[1] Matthew J. Leonardi,[1] Amod Timalsina,[1] Eric F. Manley,[1] Dugan Hayes,[2] Joseph Strzalka,[3] Mark C. Hersam,[1,4] Robert P.H. Chang,[4] Tobin J. Marks[1]*, Lin X. Chen[1,2]*

[1]Department of Chemistry, Northwestern University, Evanston, Illinois 60208, USA

[2]Chemical Science and Engineering Division, [3]X-ray Science Division, Advanced Photon Source, Argonne National Laboratory, Lemont, Illinois 60439, USA

[4]Department of Materials Science and Engineering, Northwestern University, Evanston, Illinois 60208, USA

1. *Grazing incidence x-ray scattering*

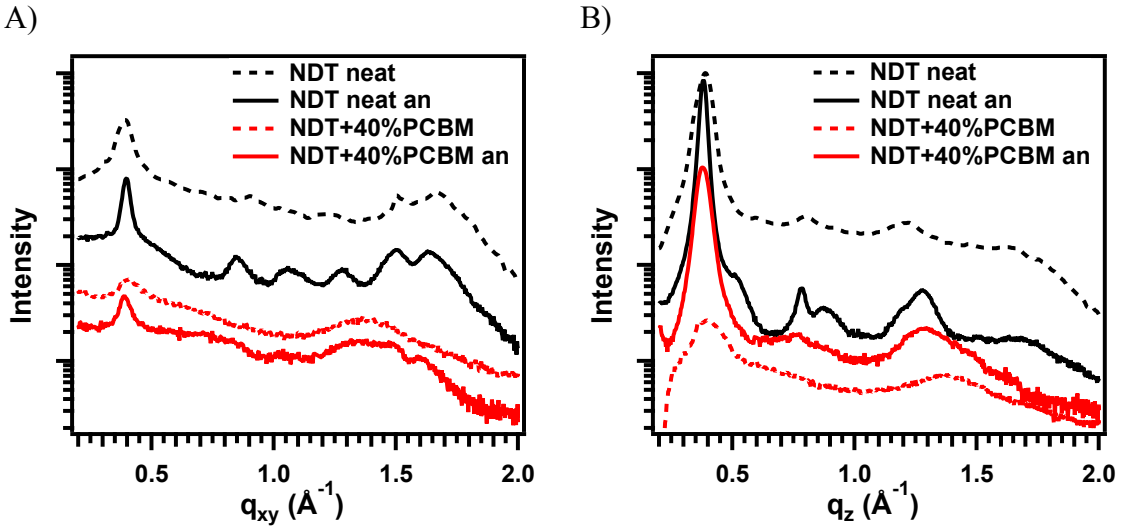

Figure S1. A) In-plane and B) out of plane scattering of neat and NDT+40%PCBM ratios unannealed or annealed at 150°C.

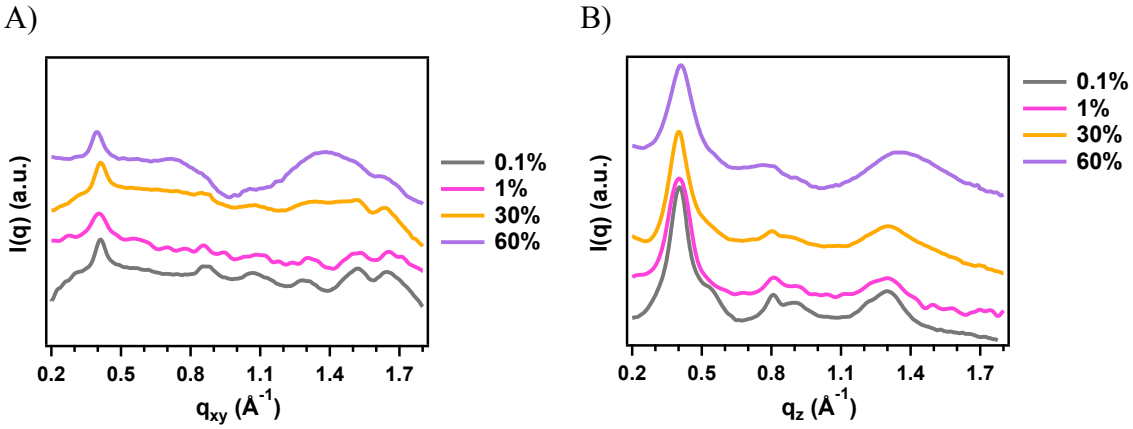

Figure S2. A) Out-of-plane and B) in-plane scattering of NDT with PCBM loadings not shown in the main text (0.1%, 1%, 30%, 60%) to demonstrate similarities in trends.

Table S1. Peak d-spacing and crystalline correlation lengths for in-plane diffraction peaks in the NDT crystal structure at varying loadings of PCBM and corresponding crystalline orientations.

Peak	%PCBM	*d*-spacing (Å)	CCL (Å)
(010) side-on and end-on	NDT neat an	15.2	194.3
	NDT neat no an	16.2	109.2
	10%	15.1	166.8
	20%	16.0	174.5
	30%	15.2	169.0
	40%	15.1	183.7
	40% no an	15.5	82.8
	50%	15.2	167.9
	60%	15.9	151.0
	80%	16.1	168.7
(02-1) end-on	NDT an	7.3	36.20
	NDT no an	6.9	155.49
	10%	7.4	33.09
	20%	7.5	136.05
	30%	---	---
	40%	7.2	494.84
	50%	7.4	192.96
(02-2) end-on	NDT an	5.8	44.68
	10%	6.0	60.40
	20%	5.9	46.14
(1-2-1)/(112) side-on	NDT an	4.9	37.02
	10%	4.8	24.81
(033) end-on, side-on	NDT an	4.2	63.29
	NDT no an	4.2	118.76
	10%	4.1	73.61
	20%	4.2	169.36
	30%	4.2	112.65
	40%	4.1	159.46
	50%	4.1	69.96
	60%	4.2	190.93
	80%	4.2	202.30

(1-2-4) side-on	NDT an	3.8	53.91
	NDT no an	3.8	42.06
	10%	3.8	61.68
	20%	3.9	63.62
	30%	3.8	82.04
	40%	3.8	83.67
	50%	3.8	41.50
	60%	3.8	106.35
	80%	3.9	71.49

Table S2. Peak d-spacing and crystalline correlation lengths for in-plane diffraction peaks in the NDT crystal structure at varying loadings of PCBM and corresponding crystalline orientations.

Peak	%PCBM	d-spacing (Å)	CCL (Å)
(001) side-on and end-on	NDT an	15.6	211.96
	NDT no an	16.3	100.28
	10%	15.6	211.44
	20%	15.6	143.38
	30%	15.7	194.24
	40%	15.6	160.98
	40% no an	15.6	49.94
	50%	15.7	152.78
	60%	16.4	132.74
	80%	16.7	117.83
(01-2) side-on	NDT an	7.8	177.20
	NDT no an	7.9	46.00
	10%	7.8	225.99
	20%	8.1	228.21
(02-1) side-on	NDT an	7.0	58.67
	10%	7.1	35.30
	20%	7.1	70.56
	30%	7.1	144.61
	40%	7.0	118.00
	50%	7.1	176.44
	60%	6.9	161.68
(1-1-2) end-on	NDT an	5.0	36.48
	NDT no an	5.2	47.06
	10%	5.1	42.35
	20%	4.9	52.93
	30%	4.8	35.62
(023) end-on	NDT an	4.8	81.59
	NDT noan	4.7	157.36
	10%	4.8	58.28
	20%	4.7	16.94
	30%	4.8	35.62
	40%	4.8	104.85

2. UV-Vis absorption

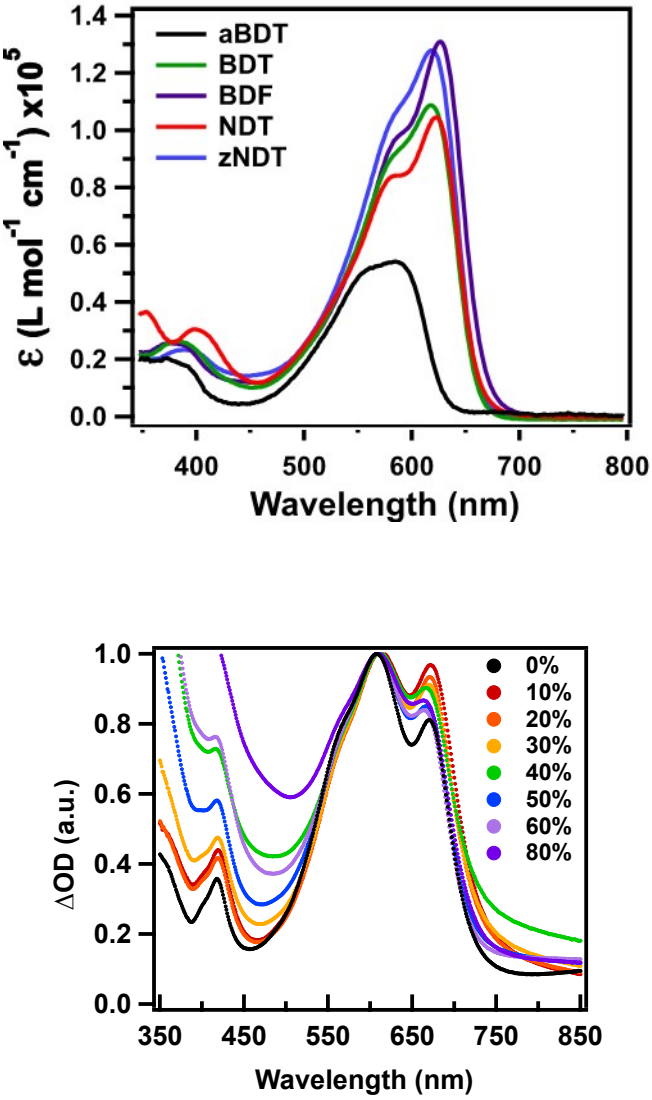

Figure S3. UV-Vis absorption of NDT in CHCl3 solution (top) and NDT:PCBM films with varying PCBM loadings (bottom). The top figure is extracted from a previous publication[1] with NDT (red curve) among other spectra.

3. Transient absorption spectroscopy

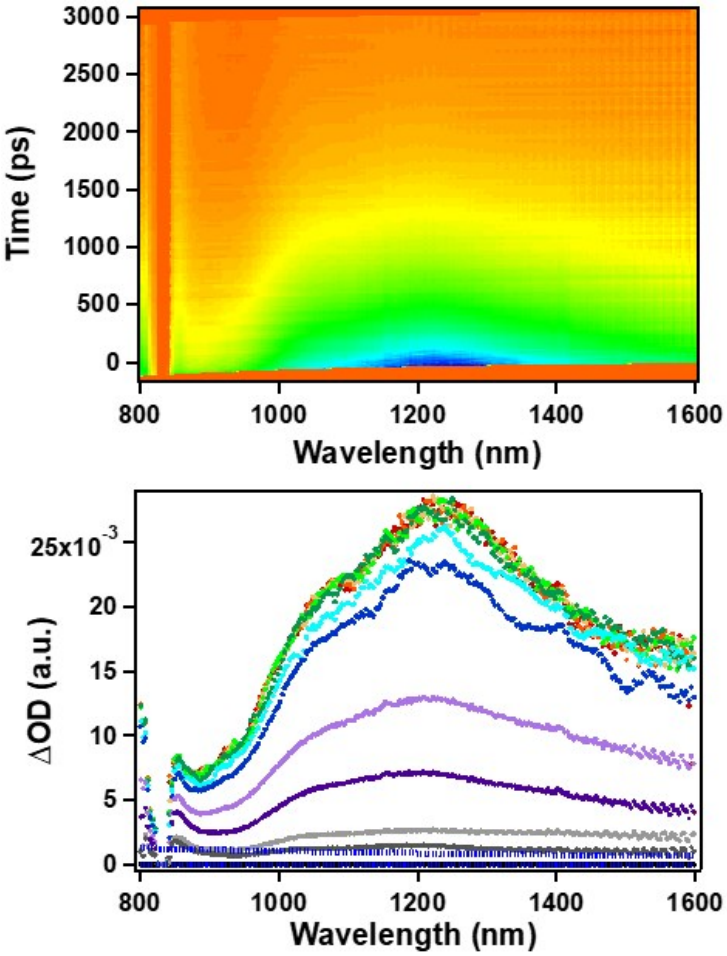

Figure S4. TA spectra of NDT in $CHCl_3$. Top: Two dimensional full TA contour with probe wavelength and delay time; Bottom: TA absorption in NIR region at different delays from 0 – 3 ns extracted from the top contour map.

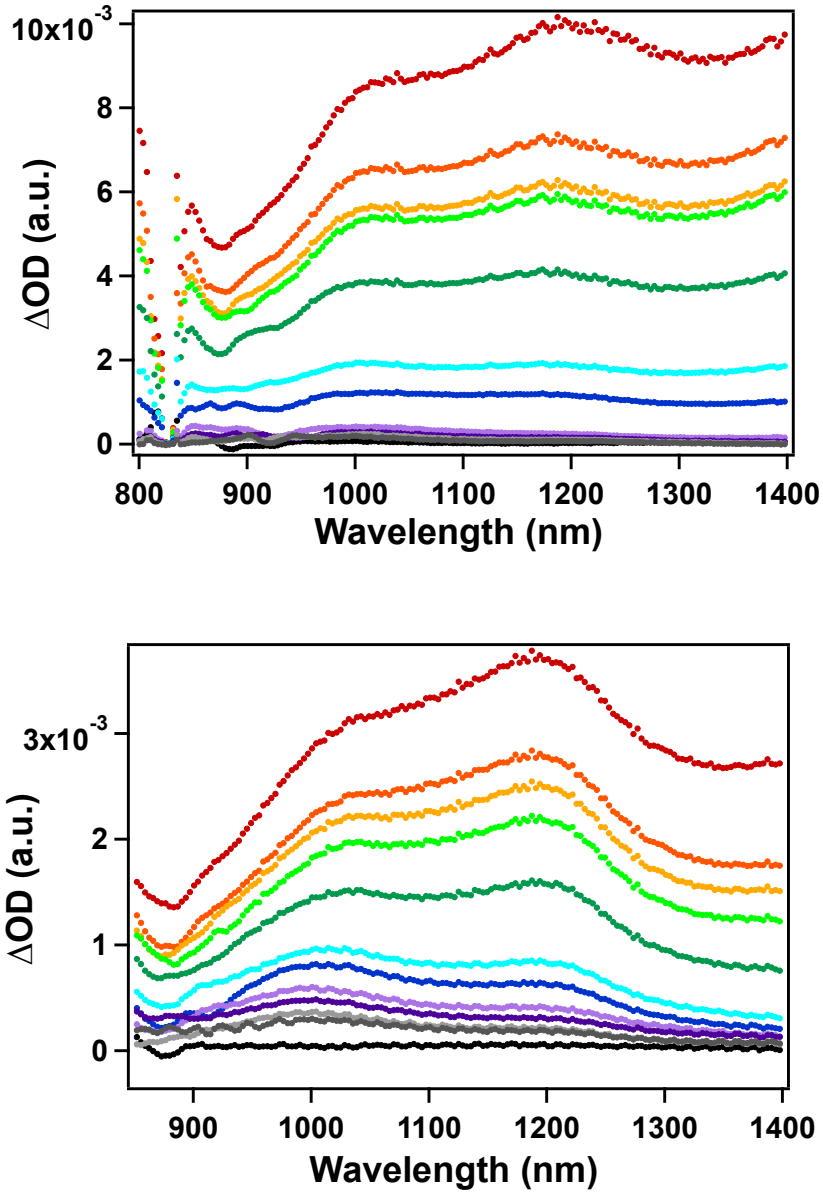

Figure S5. TA spectra of NDT in the 0-3 ns pump-probe delay time window. Top: Neat NDT film, and Bottom: BHJ film with 40% $PC_{61}BM$ loading.

Table S3. EX state decay dynamics for all NDT+PCBM films from transient absorption. *unannealed films

% PCBM	t_1 (ps)	t_2 (ps)	t_3 (ps)	A_1 ($x10^{-4}$)	A_2 ($x10^{-4}$)	A_3 ($x10^{-4}$)
0	7.1 (0.3)	105.6 (4.6)	>3000	6.8 (0.2)	7.5 (0.2)	2.1 (0.1)
0*	2.5 (0.1)	54.1 (2.3)	1829 (303)	20 (0.6)	18 (0.4)	0.2 (0.2)
0.1	6.2 (1.1)	58.6 (11.3)	---	7.3 (0.7)	4.7 (0.7)	---
1	6.0 (0.4)	88.0 (4.7)	---	7.8 (0.2)	5.5 (0.2)	---
10	7.8 (0.4)	91.2 (5.4)	2240 (145)	5.5 (0.2)	6.4 (0.2)	2.4 (0.1)
20	6.1 (0.6)	82.2 (7.8)	2365 (237)	7.6 (0.5)	8.1 (0.4)	2.7 (0.2)
30	8.6 (0.5)	102.7 (5.5)	>3000	11 (0.3)	10 (0.3)	4.0 (0.1)
40	6.9 (0.2)	96.3 (4.3)	2240 (111)	5.5 (0.1)	5.1 (0.1)	1.4 (0.1)
40*	4.9 (0.2)	75.9 (5.1)	>3000	15 (0.3)	8.3 (0.3)	4.4 (0.2)
50	10.9 (0.9)	162.6 (22.6)	>3000	12 (0.4)	5.5 (0.4)	2.1 (0.1)
60	8.7 (0.8)	124.6 (14.6)	>3000	8.5 (0.3)	5.1 (0.3)	2.2 (0.1)
80	5.8 (0.4)	85.6 (7.5)	>3000	7.2 (0.3)	7.0 (0.3)	2.1 (0.1)

(1) Loser, S.; Lou, S. J.; Savoie, B. M.; Bruns, C. J.; Timalsina, A.; Leonardi, M. J.; Smith, J.; Harschneck, T.; Turrisi, R.; Zhou, N.; Stern, C. L.; Sarjeant, A. A.; Facchetti, A.; Chang, R. P. H.; Stupp, S. I.; Ratner, M. A.; Chen, L. X.; Marks, T. J. Systematic evaluation of structure-property relationships in heteroacene - diketopyrrolopyrrole molecular donors for organic solar cells. *Journal of Materials Chemistry A* **2017**, *5*, 9217-9232.